

Katherine A. Henzler Wildman<sup>1</sup>

Dong-Kuk Lee<sup>2</sup>

A. Ramamoorthy<sup>1,2,3</sup>

<sup>1</sup> Department of Chemistry,  
University of Michigan,  
Ann Arbor, MI 48109-1055

<sup>2</sup> Biophysics Research Division,  
University of Michigan,  
Ann Arbor, MI 48109-1055

<sup>3</sup> Macromolecular Science  
and Engineering,  
University of Michigan,  
Ann Arbor, MI 48109-1055

Received 25 October 2001;  
accepted 27 March 2002

## Determination of $\alpha$ -Helix and $\beta$ -Sheet Stability in the Solid State: A Solid-State NMR Investigation of Poly(L-Alanine)

**Abstract :** The relative stability of  $\alpha$ -helix and  $\beta$ -sheet secondary structure in the solid state was investigated using poly(L-alanine) (PLA) as a model system. Protein folding and stability has been well studied in solution, but little is known about solid-state environments, such as the core of a folded protein, where peptide packing interactions are the dominant factor in determining structural stability. <sup>13</sup>C cross-polarization with magic angle spinning (CPMAS) NMR spectroscopy was used to determine the backbone conformation of solid powder samples of 15-kDa and 21.4-kDa PLA before and after various sample treatments. Reprecipitation from helix-inducing solvents traps the  $\alpha$ -helical conformation of PLA, although the method of reprecipitation also affects the conformational distribution. Grinding converts the secondary structure of PLA to a final steady-state mixture of 55%  $\beta$ -sheet and 45%  $\alpha$ -helix at room temperature regardless of the initial secondary structure. Grinding PLA at liquid nitrogen temperatures leads to a similar steady-state mixture with 60%  $\beta$ -sheet and 40%  $\alpha$ -helix, indicating that mechanical shear force is sufficient to induce secondary structure interconversion. Cooling the sample in liquid nitrogen or subjecting it to high pressure has no effect on secondary structure. Heating the sample without grinding results in equilibration of secondary structure to 50%  $\alpha$ -helix/50%  $\beta$ -sheet at 100°C when starting from a mostly  $\alpha$ -helical state. No change was observed upon heating a  $\beta$ -sheet sample, perhaps due to kinetic effects and the different heating rate used in the experiments. These results are consistent with  $\beta$ -sheet approximately 260 J/mol more stable than  $\alpha$ -helix in solid-state PLA. © 2002 Wiley Periodicals, Inc. *Biopolymers* 64: 246–254, 2002

**Keywords :** poly(L-alanine); solid state; NMR;  $\alpha$ -helix;  $\beta$ -sheet; secondary structure; stability; peptide

### INTRODUCTION

Protein folding and stability in solution have been studied extensively over the past 40 years. Experi-

ments with simple model systems have aided in the development of theoretical models for the folding of isolated  $\alpha$ -helices and  $\beta$ -hairpins in solution,<sup>1–4</sup> and denaturation studies have elucidated specific interme-

Correspondence to: A. Ramamoorthy; email: ramamoor@umich.edu

Contract grant sponsor: NSF  
*Biopolymers*, Vol. 64, 246–254 (2002)  
© 2002 Wiley Periodicals, Inc.

diates in the folding pathways of several small globular proteins.<sup>5–7</sup> In solution, solvent interactions dominate protein folding and stability via the hydrophobic effect. Although the initial folding of an extended polypeptide is determined by extensive interaction with water, some biological contexts contain little or no water and are better modeled as solid environments due to the dense packing of the atoms.<sup>8,9</sup> For example, the hydrophobic core of large proteins or extended protein aggregate structures, such as amyloid fibrils, are densely packed environments with peptide–peptide packing interactions replacing solvent effects as the dominant factor. However, very little is known about the relative stability and packing ability of secondary structure elements in a solid environment.

Long-range sequence-specific interactions complicate the study of secondary structure formation, stability, and packing in real proteins. Model systems allow these factors to be isolated and investigated independently. This work examines the different conformations assumed by poly(L-alanine) (PLA) in the solid state using NMR. PLA is the simplest homopolypeptide with a side chain, maintaining the L-stereochemistry shared by 19 of the 20 common amino acids. The small size of the methyl side chain of alanine allows relative conformational flexibility while retaining enough bulk to stabilize secondary structure through side-chain–side-chain van der Waals interactions,<sup>10,11</sup> and the nonpolar nature of the methyl group also eliminates side-chain electrostatic and hydrogen-bonding interactions. The use of a homopolypeptide eliminates primary sequence variation and sequence-specific interactions, and also reduces the number of stable, ordered conformations to a few regular secondary structures. X-ray diffraction data reveals that PLA assumes  $\alpha$ -helical and antiparallel  $\beta$ -sheet conformations in the solid state,<sup>12,13</sup> the two most common forms of secondary structure in proteins. Investigation of the interconversion of these two conformations provides insight into their relative stability and the external conditions that favor each conformation. PLA is particularly interesting because it has been proposed as a universal reference due to its unique characteristics,<sup>14</sup> and as a good model system for the  $\alpha$ -helix to  $\beta$ -sheet conformational transition implicated in amyloidogenesis.<sup>15</sup>

<sup>13</sup>C Cross-polarization magic angle spinning (CP-MAS) is a standard solid-state NMR method that observes isotropic chemical shift spectra of solid powder samples. The <sup>13</sup>C isotropic chemical shift depends on the backbone torsion angles and hydrogen-bonding pattern (carbonyl carbon only), resulting in a strong correlation with secondary structure.<sup>16–21</sup> <sup>13</sup>C CP-MAS of polypeptides was developed by comparing

spectra of PLA and other peptide samples with their known secondary structure (obtained from x-ray diffraction),<sup>22–25</sup> and is a well-established method for quantitative secondary structure determination in solid-state peptide and protein samples.<sup>16,24,26–28</sup> The conformation of PLA depends on the polymerization conditions used in synthesis,<sup>22,24,25</sup> and the interconversion of  $\alpha$ -helical and  $\beta$ -sheet structure in PLA was demonstrated by stretching or rolling PLA fibers in steam or with a plasticizing agent.<sup>13,29</sup> In solution NMR, certain solvents are known to induce  $\alpha$ -helical secondary structure, and this has been established for PLA as well.<sup>30–34</sup> Studies performed on polyalanine, short alanine oligomers, and alanine-rich natural peptides, such as silk, demonstrate that reprecipitation from these solvents can also induce conformational change.<sup>27,28,35–38</sup> Although previous studies identified common factors such as heat, mechanical force, and solvent interaction as possible contributors to secondary structure conversion in PLA and other peptides, none systematically investigated the interconversion of  $\alpha$ -helix and  $\beta$ -sheet structure. The results presented here build on previous work, purposefully manipulating the conformation of PLA in order to investigate the relative stability of  $\alpha$ -helix and  $\beta$ -sheet in the solid state.

## MATERIALS AND METHODS

### Sample Preparation

The 15- and 21.4-kDa PLA were purchased from Sigma Chemical Co. (St. Louis, MO) several years apart. Sigma prepares PLA using base-initiated polymerization of 4-methyl-2,5-oxazolidinedione (L-Ala NCA), although the particular initiator used varies, resulting in different secondary structure in the polymerized PLA.

**Reprecipitation.** DCA: PLA samples were dissolved in dichloroacetic acid (DCA) by adding 1–2 mL of chloroform followed by enough DCA to make a clear solution (about 15–20 mL). They were then precipitated with an equal volume of cold ether and collected by vacuum filtration.

TFA: PLA samples were similarly dissolved in trifluoroacetic acid (TFA) with a small amount of glacial acetic acid. Samples were reprecipitated with ether or the solvent was evaporated off under a steady stream of air. All samples were dried overnight under vacuum at room temperature to remove any traces of solvent and no residual solvent peaks were observed in any of the spectra.

**Pressure Treatment.** The 21.4-kDa PLA was put into a die used for making KBr pellets for Fourier transform infrared spectroscopy (FTIR) and subjected to 10 000 lbs of

pressure for 10 min. The pellet was gently broken up in a mortar and pestle to restore a uniform powder.

**Ground Samples.** The samples were ground in a Wig-L-Bug ball mill. The 60- and 90-min samples were prepared by grinding for two 30- or 45-min periods with a 10-min break in between. The samples were slightly warm to the touch after the extended grinding periods at room temperature. The cold ground samples were prepared in the same way except that the sealed ball mill chamber was submerged in liquid nitrogen for the entire grinding period to maintain a steady temperature and prevent heating of the sample.

**Cooled Samples.** PLA was added directly to about 100 mL of liquid nitrogen and recollected once all the liquid nitrogen had evaporated.

**Heated Samples.** PLA was heated in a Chemagnetics VT-MAS probe in the spectrometer. The sample and probe were equilibrated at each temperature for at least half an hour before data was collected. Acquisition time ranged from 30 min to several hours and increased with temperature as sensitivity declined. Spectra were obtained in order of increasing temperature at 37, 50, 75, 100, 120, 140, 160, and 180°C. The sample was then cooled to room temperature and no difference was observed between the spectra of the sample taken at 180°C and after cooling. Previous experiments with another PLA sample showed the same result.<sup>38</sup> Due to temperature limits of the NMR probe, heating above 180°C was done in an oven with the sample remaining at temperature for 3–4 h before it was cooled and observed at room temperature. Temperatures above 225°C resulted in decomposition of the sample.

## Viscometry

Polymer length was characterized using an Ubbelohde viscometer to measure the viscosity of 21.4-kDa commercial and 21.4-kDa ground PLA dissolved in TFA. The inherent viscosity,  $\eta_{inh}$ , was calculated using:  $\eta_{inh} = \{\ln [(t - t_0)/t_0]\}/c$ , where  $t$  is the time for a solution with concentration  $c$  (g/mL) of PLA in TFA to run through the viscometer and  $t_0$  is the time for pure TFA to run through the viscometer. The molecular weight, and therefore the length of the unbranched PLA chain, can be estimated from  $\eta_{inh}$  using several methods based on other polypeptides.<sup>39,40</sup>

## NMR Experiments

All solid-state  $^{13}\text{C}$  CPMAS experiments were performed on a Chemagnetics Infinity 400 MHz spectrometer equipped with a 9.4-T wide-bore magnet. Resonance frequencies for  $^{13}\text{C}$  and  $^1\text{H}$  nuclei were 100.62 and 400.14 MHz, respectively. CPMAS experiments were performed using a 5-mm Zirconia rotor in a Chemagnetics triple resonance probe.

The  $^{13}\text{C}$  CPMAS spectra were acquired using a single contact CP pulse sequence with a 2-ms contact time, a

20.5-ms acquisition time, and a 3.0- to 5.0-s recycle delay time. A radio frequency (rf) field strength of 34 kHz was used for cross-polarization and 78 kHz was used for proton decoupling. TPPM (two-pulse phase modulation)<sup>41</sup> was used for  $^1\text{H}$  decoupling during acquisition of the spectra and samples were spun at the magic angle at  $7\text{--}10 \pm 0.001$  kHz. The  $^1\text{H}$  90° pulse length was 3.1–3.4  $\mu\text{s}$  in all of the CPMAS experiments. Adamantane was used to shim the magnet, set the experimental conditions, and reference the  $^{13}\text{C}$  spectra relative to tetramethyl silane (TMS) at 0 ppm (adamantane, 29.5 and 38.6 ppm). The spectra were processed on a Sun Spare computer using Chemagnetics' Spinsight software. The FIDs (free induction decays) were apodized using 20-Hz exponential broadening and zero filled to 8192 points. The Fourier transformed data was then phased and referenced.

The percentage of  $\alpha$ -helix and  $\beta$ -sheet in each sample was determined by comparing the relative peak height due to each conformation in the  $^{13}\text{C}=\text{O}$  and  $^{13}\text{C}_\alpha$  regions of the CPMAS spectrum.<sup>24</sup> Similar results were obtained when the areas of fit peaks in deconvoluted spectra were used to calculate the amount of  $\alpha$ -helix and  $\beta$ -sheet. The composition determined from the  $^{13}\text{C}=\text{O}$  and  $^{13}\text{C}_\alpha$  peaks always agreed within 2%, and their average is reported here. The  $^{13}\text{C}_\beta$  peaks were not used because the location of  $^{13}\text{C}_\beta$  in the side chain makes it sensitive to side-chain torsion angle, leading to broader, less well-resolved peaks, although it is always in qualitative agreement with  $^{13}\text{C}=\text{O}$  and  $^{13}\text{C}_\alpha$ . The error in the quantitation of secondary structure was estimated at 2% by comparing the conformation determined from both the  $^{13}\text{C}_\alpha$  and  $^{13}\text{C}=\text{O}$  peaks of 3 separate 21.4-kDa commercial PLA samples recorded independently.

## RESULTS

The secondary structure of PLA in the solid state was determined from  $^{13}\text{C}$  CPMAS spectra of powder samples. The characteristic  $^{13}\text{C}$  isotropic chemical shift ranges for  $\alpha$ -helix and  $\beta$ -sheet conformations reported in the literature are given in Table 1<sup>21–23,25,38</sup> and average values are marked with dotted lines in Figures 1, 3 and 4. The relative intensity of the peaks corresponding to  $\alpha$ -helix and  $\beta$ -sheet secondary structure in a  $^{13}\text{C}$  CPMAS spectrum is proportional to the amount of each present in the sample<sup>24</sup> and was used to quantitatively determine the distribution of secondary structures in a sample. The samples used in this work were 15-kDa commercial PLA (Figure 1A), which is primarily  $\beta$ -sheet, and 21.4-kDa commercial PLA (Figure 1E), which is mostly  $\alpha$ -helical. It has been well established that both the polymerization conditions and the initiator used in polymerization determine the length and initial conformation of PLA.<sup>22,35</sup>

The results of reprecipitation from DCA, a helix-promoting solvent,<sup>32</sup> are shown in Figure 1. The  $^{13}\text{C}$

**Table I** Isotropic  $^{13}\text{C}$  Chemical Shift of Poly(L-Alanine) Powder Samples Characteristic of Secondary Structure as Reported in the Literature ( $\pm 0.5$  ppm from TMS)

Nucleus:	C=O		$\text{C}_\alpha$		$\text{C}_\beta$		Ref.
	$\alpha$ -Helix	$\beta$ -Sheet	$\alpha$ -Helix	$\beta$ -Sheet	$\alpha$ -Helix	$\beta$ -Sheet	
Conformation:							
Chemical shift:			53.0	48.7	15.5	21.0	21
	176.2	171.6	52.3	48.7	14.8	20.0	22
	176.8	172.2	52.8	49.3	15.5	20.3	23
	176.4	171.8	52.4	48.2	14.9	19.9	25
	175.7	173.1	53.1	49.4	16.1	20.3	38
	176.3	172.1	53.2	49.1	15.8	20.0	38
	176.2	173.1	53.5	49.9	16.1	21.6	38

CPMAS spectra of commercial 15-kDa PLA before (Figure 1A) and after (Figure 1B) reprecipitation from DCA reveal that the  $\beta$ -sheet content was greatly reduced and the final conformation was predominantly  $\alpha$ -helical. In a sample that was initially a mixture of  $\alpha$ -helix and  $\beta$ -sheet (21.4-kDa PLA ground for 10 min, Figure 1H) the amount of  $\alpha$ -helical secondary structure also increased significantly upon reprecipitation from DCA (Figure 1I). These results confirm that a solvent-induced  $\alpha$ -helical conformation may be trapped in the solid state upon reprecipitation. TFA has a different effect on PLA conformation. Comparison of spectra A and C in Figure 1 shows that reprecipitation from TFA using ether only induced a slight increase in the amount of  $\alpha$ -helix in 15-kDa PLA. Similar results were observed for 21.4-kDa PLA (Figure 1E, F). In addition to the solvent, the precipitation method also affects the final conformation of the solid sample. 21.4-kDa PLA samples reprecipitated from TFA by ether or by solvent evaporation had small but significant differences in secondary structure as can be seen in Figure 1F and 1G, respectively.

It has also been reported in the literature that  $\beta$ -sheet conformation can be induced by rolling  $\alpha$ -helical PLA fibers in damp steam or with plasticizers.<sup>13,29</sup> Heat, mechanical force, and interaction with solvent may all contribute to the conformational transition under these conditions. In order to determine which of these factors are essential, different sample preparation methods were used to isolate each of these components.  $^{13}\text{C}$  CPMAS spectra showing the results of grinding PLA for 10 min at room temperature are also shown in Figure 1. Examination of the spectra shows that the  $\beta$ -sheet content increased significantly in the initially  $\alpha$ -helical 21.4-kDa PLA sample after 10 min of grinding (Figure 1E, H). However, the opposite effect was observed when a mainly  $\beta$ -sheet sample (15-kDa PLA reprecipitated from TFA) was

ground for 10 min. (Figure 1C, D). The induction of  $\alpha$ -helix in a primarily  $\beta$ -sheet sample as the result of grinding was confirmed with a second sample of 15-kDa commercial PLA (spectra not shown). Unlike solvent interactions, grinding does not favor  $\alpha$ -helix or  $\beta$ -sheet, but leads to a steady-state mixture of  $\alpha$ -helix and  $\beta$ -sheet regardless of the initial sample conformation as summarized in Figure 2A.

The initial grinding experiments were performed at room temperature and samples were warm to the touch after being ground since no effort was made to limit heating due to friction. Thus, the changes in secondary structure observed upon grinding in the ball mill may be the result of the pressure of impact, mechanical shear force, or increased temperature, and experiments were performed to isolate these factors. Spectra of 21.4-kDa PLA before and after subjecting the sample to 10 000 lbs of pressure for 10 min were identical (spectra not shown). Since pressure alone caused no change in conformation, the closeness of packing of the  $\alpha$ -helix and  $\beta$ -sheet forms must be comparable, so that neither form is strongly favored under the pressures tested. In order to isolate mechanical shear force, grinding was performed at liquid nitrogen temperatures. To confirm that cooling the sample in liquid nitrogen had no effect of its own, spectra of several PLA samples were compared before and after submersion in liquid nitrogen and no change was observed (spectra not shown). As can be seen in Figure 2B, however, grinding the samples at liquid nitrogen temperatures did cause the secondary structure of the sample to change so that a steady-state mixture of  $\alpha$ -helix and  $\beta$ -sheet was obtained upon grinding for long periods, regardless of the initial sample conformation. This demonstrates that mechanical force is sufficient for secondary structure interconversion in solid-state PLA.

The effect of heat on a mostly  $\alpha$ -helical sample (15-kDa PLA after reprecipitation from DCA) was

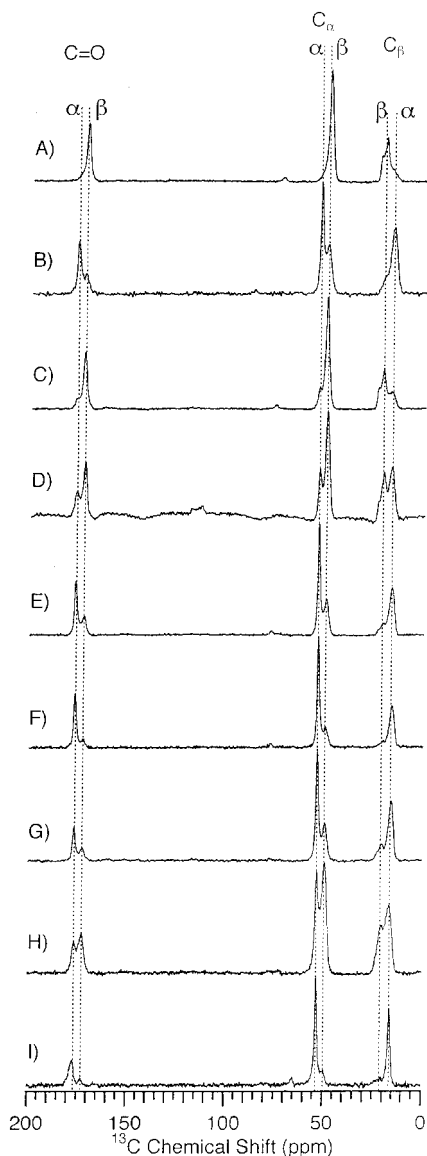


**FIGURE 1**  $^{13}\text{C}$  CPMAS spectra of PLA powder samples: Effect of solvent reprecipitation and grinding on solid PLA conformation. (A) 15-kDa commercial PLA; (B) 15-kDa PLA reprecipitated from DCA; (C) 15-kDa PLA reprecipitated from TFA with ether; (D) 15-kDa PLA reprecipitated from TFA then ground 10 min; (E) 21.4-kDa commercial PLA; (F) 21.4-kDa PLA reprecipitated from TFA with ether; (G) 21.4-kDa PLA reprecipitated from TFA by solvent evaporation; (H) 21.4-kDa PLA ground 10 min; (I) 21.4-kDa PLA ground 10 min. then reprecipitated from DCA. The dotted lines labeled  $\alpha$  and  $\beta$  indicate the chemical shifts characteristic of  $\alpha$ -helix and  $\beta$ -sheet, respectively. The amount of each type of secondary structure present in the sample is reflected in the peak intensities.

reported previously.<sup>38</sup> In that work, the secondary structure composition of the sample underwent a transition centered slightly above 100°C and reequili-

brated to a mixture with nearly 50%  $\alpha$ -helix and 50%  $\beta$ -sheet. However, when a primarily  $\beta$ -sheet sample (15-kDa PLA) was heated (Figure 3), only slight line broadening was observed. There was no change in conformation up to 225°C and further heating of the sample was not possible because of PLA decomposition. This difference in behavior of  $\alpha$ -helical and  $\beta$ -sheet PLA upon heating may be caused by kinetic effects since the samples were heated at different rates. Thus, temperature may induce secondary structure interconversion, but mechanical shear force is a method that avoids high temperature decomposition and kinetic limitations.

Additional experiments were done to confirm that the observed spectral changes resulted from conformational conversion between  $\alpha$ -helix and  $\beta$ -sheet and not from fragmentation of the polypeptide backbone. The viscosity of 21.4-kDa PLA ground for 30 min and commercial 21.4-kDa PLA dissolved in TFA was found to be the same (0.35 dL/g), demonstrating that the molecular weight distribution of the PLA sample was not significantly altered by grinding. In addition, the spectra of oligo-L-alanines (trimer, tetramer, pentamer) are given in Figure 4, and the effects of the peptide termini are visible in the multiple resolved peaks in each region of the spectrum. As the length of the oligomer increases, more residues are further removed from the endgroups, and the well-resolved oligomer peaks begin to coalesce into a more poly(L-alanine)-like spectrum where the chemical shift is determined by conformation and end effects are negligible. The spectra of ground PLA samples do not show any sharp, well-resolved peaks indicative of oligomers, demonstrating that the poly(L-alanine) character is maintained and that small fragments with chemical shifts altered by proximity to end groups are not formed in significant numbers in the sample. Reprecipitation from DCA of 21.4-kDa PLA that had been ground for 10 min resulted in an increased  $\alpha$ -helical content (Figure 1H, I), providing additional evidence that grinding does not cause an irreversible change in the sample as would be expected if covalent bonds were broken. These results rule out significant backbone fragmentation.

## DISCUSSION

The pattern of changes observed in the  $^{13}\text{C}$  CPMAS spectra upon grinding are not consistent with the formation of  $3_{10}$ -helix, random coil, or other structural alterations in the sample, and must result from interconversion of  $\alpha$ -helix and  $\beta$ -sheet. Induction of random coil structure by mechanical deformation of

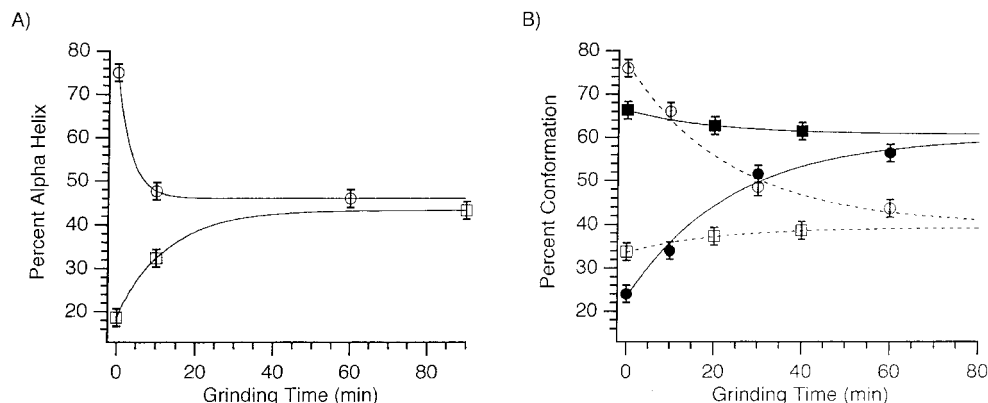


**FIGURE 2** Equilibration of secondary structure as a result of grinding PLA. (A) *Room temperature*. The graph shows the percentage of  $\alpha$ -helix present in each PLA sample as a function of grinding time at approximately room temperature. Two different samples of PLA with different initial conformations were used: 21.4-kDa commercial PLA (circles), and 15-kDa PLA reprecipitated from TFA with ether (squares). (B) *Liquid nitrogen temperature*. The percentage of  $\alpha$ -helix (open symbols, dotted lines) and  $\beta$ -sheet (solid symbols, solid lines) in each sample is shown in the graph. Two different samples of PLA were again used: 21.4-kDa commercial PLA (circles), and 15-kDa PLA reprecipitated from TFA and previously ground 10 min. at room temperature (squares). The conformations were determined from  $^{13}\text{C}$  CPMAS spectra recorded after each period of grinding and error bars of  $\pm 2\%$  represent the error in secondary structure determination based on repeated analysis of identical samples.

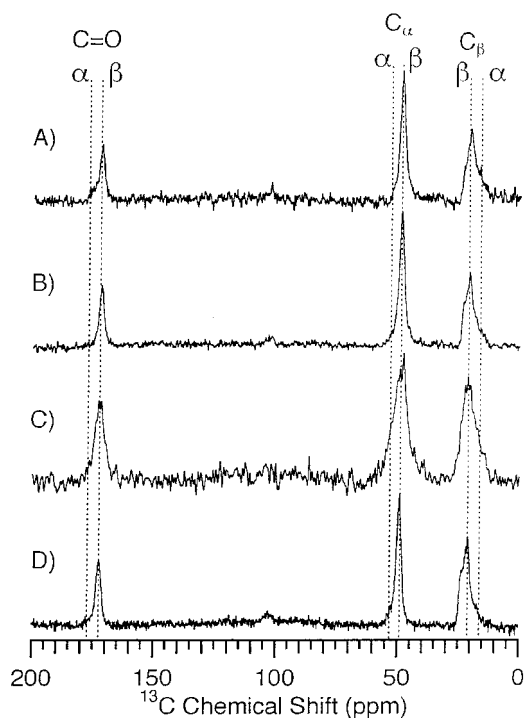


**FIGURE 3** Effect of heating on  $\beta$ -sheet structure.  $^{13}\text{C}$  CPMAS spectra of 15-kDa PLA. (A) 37 °C; (B) 100°C; (C) 160°C; (D) quickly cooled after heating at 225°C for 3 h in the oven.

PLA has been suggested on the basis of Raman spectroscopic studies of stretched PLA fibers.<sup>29</sup> Random coil chemical shifts for various amino acid residues in solution have been published,<sup>42</sup> but random coil conformation in solution is defined by extensive solvent interactions which are not present in the solid state. Neglecting this due to the absence of data in the solid state, and assuming that the random coil conformations determined in solution are also valid for solids, the characteristic chemical shifts for an alanine residue in a polypeptide chain are 177.8, 52.5, and 19.1 ppm. This  $^{13}\text{C}=\text{O}$  shift is slightly higher than that typical of either secondary structure, the  $^{13}\text{C}_\alpha$  shift is in the typical  $\alpha$ -helical range, and the  $^{13}\text{C}_\beta$  shift is slightly below the typical  $\beta$ -sheet range. These random coil shifts would be difficult to resolve from the secondary structure peaks, but the changes upon grinding would be distinctive since increased random coil would lead to an observed increase in  $\alpha$ -helix according to  $^{13}\text{C}=\text{O}$  and  $^{13}\text{C}_\alpha$  but an increase in  $\beta$ -sheet according to  $^{13}\text{C}_\beta$ . This was not observed. Random coil in a solid can better be defined by backbone torsion angles not characteristic of  $\alpha$ -helix or  $\beta$ -sheet structure.<sup>29</sup> In this case, an increase in intensity at chemical shifts other than the typical  $\alpha$ -helix and  $\beta$ -sheet frequencies should be observed. A slight broadening of the peaks does occur, but the spectra show only two well-defined peaks at the characteristic  $\alpha$ -helix and  $\beta$ -sheet frequencies even after

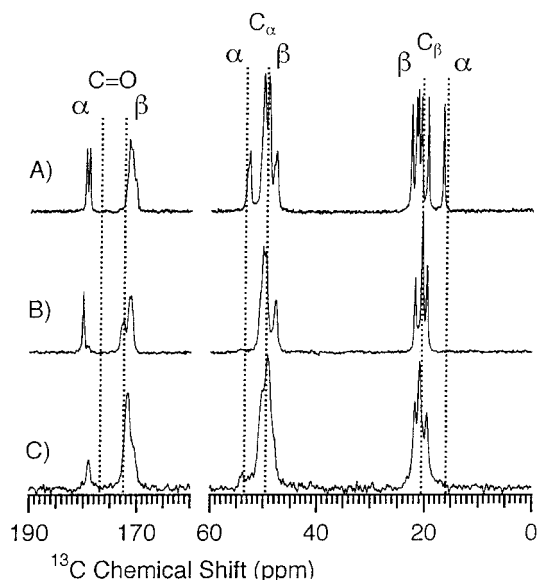


**FIGURE 4**  $^{13}\text{C}$  CPMAS spectra of oligo(L-alanines). (A) Tri-L-alanine (there are 2 inequivalent peptides per unit cell<sup>36</sup>); (B) tetra-L-alanine; (C) penta-L-alanine. The short length of the oligomers and the close proximity of all the residues to the charged end groups lead to the increased resolution and chemical shift dispersion.

extended grinding, and peaks are never observed at  $^{13}\text{C}$  isotropic chemical shifts other than those assigned to  $\alpha$ -helix and  $\beta$ -sheet.

The induction of both  $\alpha$ -helix and  $\beta$ -sheet secondary structure, as evidenced by the increase in intensity at either the  $\alpha$ -helix or  $\beta$ -sheet characteristic chemical shift depending on the initial conformation, also provides support that grinding does not cause other types of structural change. Induction of a third conformation (such as  $3_{10}$ -helix or a non- $\beta$ -sheet extended structure) upon grinding is ruled out since this would cause an increase in intensity at the same  $^{13}\text{C}$  isotropic chemical shift characteristic of that conformation in all samples. Similarly, if the effects of grinding were merely due to decreased particle size, the same trend of spectral changes (for example, a shift toward upfield peak intensity at  $^{13}\text{C}=\text{O}$ ) should have been observed in all samples as grinding time increased. Instead, an increase in the upfield ( $\beta$ -sheet)  $^{13}\text{C}_{\alpha}$  and  $^{13}\text{C}=\text{O}$  peaks occurred when the  $\alpha$ -helical 21.4-kDa commercial PLA sample was ground and an increase in the downfield ( $\alpha$ -helix)  $^{13}\text{C}_{\alpha}$  and  $^{13}\text{C}=\text{O}$  peak intensities occurred when the primarily  $\beta$ -sheet 15-kDa sample was ground (Figure 1C,D,E,H). Thus, the changes observed in the  $^{13}\text{C}$  CPMAS spectra upon grinding PLA are best explained by interconversion between  $\alpha$ -helical and  $\beta$ -sheet secondary structure.

The results presented here demonstrate that there are two fundamentally different mechanisms for in-

ducing structural change in solid PLA because of key differences between solution and solid environments. Conformational change may be mediated either by interaction with other molecules, as occurs when the peptide is dissolved in solution, or by adding energy in the form of heat or mechanical force while remaining in the solid state. In a solution environment, solvent interactions replace peptide-peptide packing, changing the energy landscape and favoring a particular peptide conformation based on the balance of intrapeptide and peptide-solvent interactions. All experimental studies of PLA in solution find it to be either  $\alpha$ -helical or random coil<sup>30-34</sup> and theoretical calculations predict  $\alpha$ -helix to be a lower energy conformation than  $\beta$ -sheet or hairpin for isolated PLA molecules surrounded by model solvents with a range of dielectric constants.<sup>10,11,43</sup> The results of reprecipitation of PLA from DCA confirm that this helical conformation may be trapped in the solid state by reprecipitation of PLA from a helix-inducing solvent (Figure 1A,B,H,I). However, this study shows that  $\alpha$ -helix may not be the most stable structure in the solid state.

Polypeptide conformation may be changed in the solid state by applying mechanical shear force or heat. Of the two methods, mechanical shear force is more effective at inducing structural change from any initial conformation (Figure 1C,D,E,H), whereas heat was only observed to affect samples that were initially  $\alpha$ -helical (Figure 3 and Ref. <sup>37</sup>). This may be a result of the interplay of kinetic and thermodynamic factors during heating since the experiments with  $\alpha$ -helical and  $\beta$ -sheet samples were performed separately with different heating rates. All the experiments reported here were performed with dry powders, ruling out the need for steam or plasticizing solvents. These results confirm a hypothesis that had been suggested previously: when mostly  $\alpha$ -helical PLA fibers are stretched or rolled in steam or plasticizers to convert them to  $\beta$ -sheet form, mechanical shear force is the primary impetus for the structural change.<sup>13,29</sup>

It is interesting to note that grinding eventually allows the sample to reach a steady-state mixture of  $\alpha$ -helix and  $\beta$ -sheet as shown in Figure 2. This may be a nonequilibrium steady state formed under the conditions of mechanical shear force that remains trapped in that conformation after the force is removed. However, this may be an equilibrium steady state because of the short duration of impact in the ball mill. An equilibrium steady state will be achieved if the sample equilibrates to its final fold under unstressed conditions after being activated by the shear forces present during grinding. Assuming, for simplicity, that an equilibrium steady state is reached, it is

possible to estimate the free energy difference between  $\alpha$ -helix and  $\beta$ -sheet conformations in the solid state from the equilibrium ratio of these secondary structures in each sample. Based on the 60%  $\beta$ -sheet/40%  $\alpha$ -helix obtained upon grinding in a liquid nitrogen bath where the temperature is controlled (Figure 2B),  $\Delta G = -260$  J/mol for the conversion of  $\alpha$ -helix to  $\beta$ -sheet. This leads to the prediction of 53%  $\beta$ -sheet/47%  $\alpha$ -helix at equilibrium at slightly above room temperature (300 K), which is consistent with the unthermostated room temperature grinding experiments (Figure 2A). At 110°C, the equilibrium would then be 51%  $\beta$ -sheet/49%  $\alpha$ -helix, which also agrees within error with the equilibrium mixture obtained by Lee et al.<sup>38</sup> upon heating an  $\alpha$ -helical PLA sample. This consistent trend in the steady-state mixture of secondary structures obtained at different temperatures supports the assumption of equilibrium. The results presented here for well-ground samples indicate that  $\alpha$ -helix and  $\beta$ -sheet have very similar free energies as expected based on theory and their ubiquitous presence in peptides and proteins, but that  $\beta$ -sheet is slightly more stable for solid-state PLA. The increase in  $\beta$ -sheet secondary structure frequently observed when amyloidogenic and prion proteins undergo the transition from soluble monomers to the insoluble fibrillized form suggests that this slight difference in secondary structure relative stability between aqueous and solid environments may play a role in some finely balanced biological systems.

## CONCLUSION

The relative stability of  $\alpha$ -helix and  $\beta$ -sheet in solid-state PLA was investigated using  $^{13}\text{C}$  CPMAS NMR and a variety of techniques to induce changes in secondary structure. PLA reprecipitated from a helix-inducing solvent retains the  $\alpha$ -helical conformation induced by the solvent, although the degree of  $\alpha$ -helical secondary structure trapped in the solid state is also influenced slightly by the method of reprecipitation. The mechanical shear force of grinding in a ball mill converts the secondary structure of all PLA samples to a steady-state mixture of  $\alpha$ -helix and  $\beta$ -sheet regardless of the initial sample conformation. The final mixture of secondary structures produced by grinding is 55%  $\beta$ -sheet/45%  $\alpha$ -helix at room temperature and 60%  $\beta$ -sheet/40%  $\alpha$ -helix at liquid nitrogen temperatures. Heating can also lead to equilibration of the secondary structure of a PLA sample that is initially  $\alpha$ -helical; however, the low sample decomposi-

tion temperature can interfere with heat induced conformational conversion. These results indicate that  $\beta$ -sheet secondary structure is slightly more stable than  $\alpha$ -helix in solid-state PLA, and are in contrast to the solution environment where  $\alpha$ -helix is favored.

This research was supported by funds from NSF (CAREER development award to A. Ramamoorthy). K. Henzler Wildman is a Howard Hughes Medical Institute Predoctoral Fellow.

## REFERENCES

1. Sun, J. K.; Doig, A. J. *J Phys Chem B* 2000, 104, 1826–1836.
2. Zimm, B. H.; Bragg, J. K. *J Chem Phys* 1959, 31, 526–535.
3. Bloomfield, V. A. *Am J Phys* 1999, 67, 1212–1215.
4. Jang, H.; Hall, C. K.; Zhou, Y. Q. *Biophys J* 2002, 82, 646–659.
5. Kuwata, K.; Shastry, R.; Cheng, H.; Hoshino, M.; Batt, C. A.; Goto, Y.; Roder, H. *Nat Struct Biol* 2001, 8, 151–155.
6. Matagne, A.; Dobson, C. M. *Cell Mol Life Sci* 1998, 54, 363–371.
7. Capaldi, A. P.; Shastry, M. C. R.; Kleanthous, C.; Roder, H.; Radford, S. E. *Nature Struct Biol* 2001, 8, 68–72.
8. Richards, F. M. *J Mol Biol* 1974, 82, 1–14.
9. Chothia, C. *Nature* 1975, 254, 304–308.
10. Yang, A. S.; Honig, B. *J Mol Biol* 1995, 252, 351–365.
11. Yang, A. S.; Honig, B. *J Mol Biol* 1995, 252, 366–376.
12. Arnott, S.; Wonacott, A. J. *J Mol Biol* 1966, 21, 371–383.
13. Arnott, S.; Dover, S. D.; Elliott, A. *J Mol Biol* 1967, 30, 201–208.
14. Head-Gordon, T.; Stillinger, F. H.; Wright, M. H.; Gay, D. M. *Proc Natl Acad Sci USA* 1992, 89, 11513–11517.
15. Blondelle, S. E.; Forood, B.; Houghten, R. A.; Perez-Paya, E. *Biochemistry* 1997, 36, 8393–8400.
16. Saito, H. *Magn Reson Chem* 1986, 24, 835–852.
17. Oldfield, E. *J Biomol NMR* 1995, 5, 217–225.
18. Wishart, D. S.; Sykes, B. D.; Richards, F. M. *J Mol Biol* 1991, 222, 311–333.
19. Wishart, D. S.; Sykes, B. D. *J Biomol NMR* 1994, 4, 171–180.
20. de Dios, A. C.; Oldfield, E. *Solid State Nucleic Magn Reson* 1996, 6, 101–125.
21. Ando, I.; Kameda, T.; Asakawa, N.; Kuroki, S.; Kurosuo, H. *J Mol Struct* 1998, 441, 213–230.
22. Kricheldorf, H. R.; Mutter, M.; Maser, F.; Muller, D.; Forster, H. *Biopolymers* 1983, 22, 1357–1372.
23. Kricheldorf, H. R.; Muller, D. *Macromolecules* 1983, 16, 615–623.



24. Muller, D.; Kricheldorf, H. R. *Polym Bull* 1981, 6, 101–108.
25. Saito, H.; Tabeta, R.; Shoji, A.; Ozaki, T.; Ando, I. *Macromolecules* 1983, 16, 1050–1057.
26. Tuzi, S.; Naito, A.; Saito, H. *Eur J Biochem* 1993, 218, 837–844.
27. Saito, H.; Tuzi, S.; Naito, A. In *Annual Reports on NMR Spectroscopy*; Webb, G. A., Ed.; Academic Press: London, 1998; Vol 36, pp 79–121.
28. Saito, H.; Ando, I. In *Annual Reports on NMR Spectroscopy*; Webb, G. A., Ed.; Academic Press: London, 1989; Vol 21, pp 209–290.
29. Frushour, B. G.; Koenig, J. L. *Biopolymers* 1974, 13, 455–474.
30. Kricheldorf, H. R. *Makromol Chem* 1979, 180, 2387–2398.
31. Shoji, A.; Kawai, T.; Nishioka, A. *Makromol Chem* 1978, 179, 611–624.
32. Shoji, A.; Kawai, T.; Nishioka, A. *Macromolecules* 1977, 10, 1292–1298.
33. Forsythe, K. H.; Hopfinger, A. J. *Macromolecules* 1973, 6, 423–437.
34. Andersen, N. H.; Dyer, R. B.; Fesinmeyer, R. M.; Gai, F.; Liu, Z. H.; Neidigh, J. W.; Tong, H. *J Am Chem Soc* 1999, 121, 9879–9880.
35. Fujie, A.; Komoto, T.; Oya, M.; Kawai, T. *Makromol Chem* 1973, 169, 301–321.
36. Hempel, A.; Camerman, N.; Camerman, A. *Biopolymers* 1991, 31, 187–192.
37. Asakura, T.; Kuzuhara, A.; Tabeta, R.; Saito, H. *Macromolecules* 1985, 18, 1841–1845.
38. Lee, D. K.; Ramamoorthy, A. *J Phys Chem B* 1999, 103, 271–275.
39. Rao, M. V. R.; Atreyi, M.; Ray, A. R. *J Macromol Sci Chem* 1977, A11, 1759–1769.
40. Brack, A.; Trudelle, Y. *Polym Commun* 1985, 26, 369–370.
41. Bennett, A. E.; Rienstra, C. M.; Auger, M.; Lakshmi, K. V.; Griffin, R. G. *J Chem Phys* 1995, 103, 6951–6958.
42. Wishart, D. S.; Bigam, C. G.; Holm, A.; Hodges, R. S.; Sykes, B. D. *J Biomol NMR* 1995, 5, 332–332.
43. Velikson, B.; Bascle, J.; Garel, T.; Orland, H. *Macromolecules* 1993, 26, 4791–4799.